

## 9. DATA REPORT: TRACE ELEMENTS AND ISOTOPES IN PORE WATER FROM SITES 1023 THROUGH 1032, EASTERN FLANK OF THE JUAN DE FUCA RIDGE<sup>1</sup>

Michael J. Mottl,<sup>2</sup> C. Geoffrey Wheat,<sup>3</sup> Christophe Monnin,<sup>4</sup> and Harry Elderfield<sup>5</sup>

### INTRODUCTION

Pore water was collected from each of 10 sites during Ocean Drilling Program (ODP) Leg 168 on the eastern flank of the Juan de Fuca Ridge. These ten sites delineate a transect perpendicular to the present ridge axis and span a crustal age of 0.86–3.59 Ma. At nine of the ten sites the entire sediment section, which ranged from 41.3 to 613.8 m thick, was cored and attempts were made to recover at least one whole round of sediment per section of core for extraction of pore water. Several (2–5) whole-round sediment samples were taken from the uppermost and lowermost cores to constrain the chemical gradient near the sediment/water and sediment/basalt interfaces, respectively.

Pore water was extracted from whole-round sediment core sections by squeezing only the most pristine sediment in a titanium squeezer designed by Manheim and Sayles (1974). Two additional water samples were collected in situ using the water-sampler temperature probe (WSTP; Barnes, 1988). Both of these samples were collected in the cased section of the open borehole from ODP Hole 1026B. Formation fluids were flowing up the cased hole into the overlying deep seawater (Fisher et al., 1997). Detailed descriptions of the sampling methods that were used to collect fluids are given by the Shipboard Scientific Party (Davis, Fisher, Firth, et al., 1997).

An additional composition listed is that of the Baby Bare springs. Baby Bare is a basement bathymetric high that penetrates the thick turbidite sediment and rises 80 m above the surrounding turbidite plain. It is located about 6.5 km south-southwest of ODP Site 1026 (Wheat and Mottl, 1994; Mottl et al., 1998). The spring composition is a composite of 39 samples from several springs on the outcrop and extrapolated to the end-member fluid, which contained virtually no magnesium (Wheat and Mottl, in press).

We present chemical analyses for Li, Rb, F, B, Mn, Fe, Sr, and Ba, and the isotopic composition of Sr, O, H, and S in pore water from Leg 168 (Table 1; Figs. 1–3). Radiocarbon measurements are reported by Elderfield et al. (1999).

### ANALYTICAL METHODS

Li and Rb were determined by flame emission spectrometry using a standard addition method similar to that of Stoffyn-Egli (1982) on a five-fold dilution of an unacidified aliquot. We measured Li at 671.0

nm and Rb at 779.4 nm, using a 0.2-nm slit. To account for spectral interference, we measured the background intensity 0.4 nm above and below the peak intensity. The average background intensity was then subtracted from the peak intensity. Precision on replicate analyses of the International Association for the Physical Sciences of the Ocean (IAPSO) standard is 1.3% for Li and 3.8% for Rb.

B, Mn, Fe, Sr, and Ba were determined at the University of Hawaii by inductively coupled plasma-atomic emission spectrometry (ICP-AES) on acidified samples, with a precision of 2%–5%. These samples were acidified with 40  $\mu$ L of sub-boiled hydrochloric acid (6 N) per 10 mL of sample. Samples were then diluted five times with 1% sub-boiled nitric acid before being injected. Sr and Ba were also determined at Universite Paul Sabatier in Toulouse by inductively coupled plasma-mass spectrometer (ICP-MS) using Indium as an internal standard, with a precision of 3% (Freydier et al., 1995). Agreement between the two methods was generally within the stated uncertainties; values reported are means.

Fluoride was determined using a modified form of the electrode method described by Froelich et al. (1983). A fluoride-ion-selective electrode was immersed in 0.2 mL of sample that was mixed with 0.2 mL of TISAB II (Orion #94-09-09) buffer. This method suffers from an interference by magnesium. Because concentrations of magnesium differ from about 0 to 52 mmol/kg in these samples, we determined the empirical relationship between the concentration of magnesium and the extent of the interference for the entire range of magnesium concentrations. This relationship was then applied to each of the samples using the concentration of magnesium that was determined shipboard. Precision was 2%.

Sr isotopic analyses were performed at the University of Cambridge (Oyun et al., 1995). O, H, and S isotopic analyses were performed by NERC Scientific Services (NIGL Keyworth and SURRC East Kilbride/University of Arizona), using standard methods.

### ACKNOWLEDGMENTS

This research was supported by the Ocean Drilling Program and by a grant from the Joint Oceanographic Institutions U.S. Science Support Program. This is contribution number 5224 from the School of Oceanography and Earth Science and Technology of the University of Hawaii.

### REFERENCES

- <sup>1</sup>Fisher, A., Davis, E.E., and Escutia, C. (Eds.), 2000. *Proc. ODP, Sci. Results*, 168: College Station TX (Ocean Drilling Program).
- <sup>2</sup>Department of Oceanography, SOEST, 1000 Pope Road, University of Hawaii, Honolulu HI 96822, USA. mmottl@soest.hawaii.edu
- <sup>3</sup>Institute of Marine Sciences, University of Alaska Fairbanks, PO Box 475, Moss Landing CA 95039, USA.
- <sup>4</sup>Laboratoire de Geochimie, CNRS/UPS, 38 rue des Trente Six Ponts, 31400 Toulouse, France.
- <sup>5</sup>Department of Earth Sciences, University of Cambridge, Downing Street, Cambridge CB2 3EQ, United Kingdom.
- Barnes, R.O., 1988. ODP in situ fluid sampling and measurement: a new wireline tool. *In* Masche, A., Moore, J.C., et al., *Proc. ODP, Init. Repts.*, 110: College Station, TX (Ocean Drilling Program), 55–63.
- Butterfield, D.A., Nelson, B.K., Wheat, C.G., Mottl, M.J., and Roe, K.K., in press. Evidence for volcanogenic Sr in mid-ocean ridge-flank hydrothermal systems and implications for the global oceanic Sr isotopic balance. *Geochim. Cosmochim. Acta*.
- Davis, E.E., Fisher, A.T., Firth, J.V., et al., 1997. *Proc. ODP, Init. Repts.*, 168: College Station, TX (Ocean Drilling Program).

- Elderfield, H., Wheat, C.G., Mottl, M.J., Monnin, C., and Spiro, B., 1999. Fluid and geochemical transport through oceanic crust: a transect across the eastern flank of the Juan de Fuca Ridge. *Earth Planet. Sci. Lett.* 172:151–165.
- Fisher, A.T., Becker, K., and Davis, E.E., 1997. The permeability of young oceanic crust east of Juan de Fuca Ridge determined using borehole thermal measurements. *Geophys. Res. Lett.*, 24:1311–1314.
- Freydier, R., Dupre, B., and Polve, M., 1995. Analyses by inductively coupled plasma mass spectrometry of Ba concentrations in water and rock samples: comparison between isotope dilution and external calibration with or without internal standard. *Eur. Mass Spectr.*, 1:283–291.
- Froelich, P.N., Kim, K.K., Jahnke, R.J., Burnett, W.R., and Soutar, A., Deakin, M., 1983. Pore water fluoride in Peru continental margin sediments: uptake from seawater. *Geochim. Cosmochim. Acta*, 47:1605–1612.
- Manheim, F.T., and Sayles, F.L., 1974. Composition and origin of interstitial waters of marine sediments, based on deep sea drill cores. In Goldberg, E.D. (Ed.), *The Sea* (Vol. 5): *Marine Chemistry: The Sedimentary Cycle*: New York (Wiley), 527–568.
- Mottl, M.J., Wheat, C.G., Baker, E., Becker, N., Davis, E., Feely, R., Grehan, A., Kadko, D., Lilley, M., Massoth, G., Moyer, C., and Sansone, F., 1998. Warm springs discovered on 3.5 Ma oceanic crust, eastern flank of the Juan de Fuca Ridge. *Geology*, 26:51–54.
- Oyun, S., Elderfield, H., and Klinkhammer, G.P., 1995. Strontium isotopes in pore waters of east equatorial Pacific sediments: indicators of seawater advection through oceanic crust and sediments. In Piasias, N.G., Mayer, L.A., Janecek, T.R., Palmer-Julson, A., and van Andel, T.H. (Eds.), *Proc. ODP, Sci. Results*, 138: College Station, TX (Ocean Drilling Program), 813–819.
- Stoffyn-Egli, P., 1982. Conservative behavior of dissolved lithium in estuarine waters. *Estuarine Coastal Shelf Sci.*, 14:577–587.
- Wheat, C.G., and Mottl, M.G., 1994. Hydrothermal circulation, Juan de Fuca Ridge eastern flank: factors controlling basement water composition. *J. Geophys. Res.*, 99:3067–3080.
- , 2000. Composition of pore and spring waters from Baby Bare: global implications of geochemical fluxes from a ridge flank hydrothermal system. *Geochim. Cosmochim. Acta.*, 64:629–642.

Date of initial receipt: 11 December 1998

Date of acceptance: 11 November 1999

Ms 168SR-019

Table 1. Composition of pore water from Sites 1023 through 1032.

Core, section, interval (cm)	Depth (mbsf)	Li (mmol/kg)	Rb (mmol/kg)	F (mmol/kg)	B (μmol/kg)	Mn (mmol/kg)	Fe (mmol/kg)	Sr (μmol/kg)	Ba (mmol/kg)	<sup>87</sup> Sr/ <sup>86</sup> Sr	δ <sup>18</sup> O (per mil)	δD (per mil)	δ <sup>34</sup> S (per mil)
168-1023A-													
1H-1, 140-150	1.45	23.1	1.93	51.9	479	139.5	7.9	87.8	3.4				
1H-2, 140-150	2.95			39.8	492	97.6	4.7	86.4	2.9				
1H-3, 140-150	4.45	13.7	1.51	33.2	491	83.5	16.8	85.0	1.7				
1H-4, 140-150	5.95			28.8	498	37.1	32.4	86.9	1.7				
1H-5, 140-150	7.45		1.58	30.6	447	0.0	0.0	76.8	1.5				
2H-1, 140-150	10.75			35.2	482	25.0	10.2	84.8	1.7				
2H-5, 140-150	16.75	14.5	1.43	37.9	487	33.2	9.3	83.1	5.5				
3H-5, 140-150	26.25			24.7	484	26.9	9.5	79.0	7.7				
4H-5, 140-150	35.75	14.2	1.10	16.9	490	14.0	6.0	79.3	2.9				
5H-5, 140-150	45.25			13.0	451	7.9	6.5	83.8	13.0				
6H-5, 140-150	54.75	10.6	0.94	14.4	420	4.7	7.5	95.9	40.7				
7H-5, 140-150	64.25			16.6	442	5.2	4.8	95.6	30.3				
8H-5, 140-150	73.75	10.2	0.83	12.0	428	7.8	6.8	95.1	40.6				
9H-5, 140-150	82.85			7.0	426	5.0	3.5	94.3	41.0				
10H-5, 140-150	92.75	9.9	0.93	10.3	389	12.2	6.5	98.4	52.3				
11H-5, 140-150	102.25			8.5	427	7.1	9.8	98.1	38.8				
12H-5, 140-150	111.75	10.3	0.88	5.9	414	11.3	7.2	98.8	45.4				
13H-5, 140-150	121.25			7.1	345	4.5	5.3	95.3	52.3				
14H-4, 140-150	129.25	9.9	0.54	7.1	422	6.2	6.1	96.1	40.2				
15X-2, 135-150	132.93	10.2	0.59	6.9	367	4.2	1.4	93.2	31.1				
16X-3, 135-150	137.13			3.9	339	9.8	5.2	89.4	35.4				
17X-3, 135-150	146.73	11.6	0.64	3.4	307	9.3	10.5	94.2	37.2				
18X-4, 135-150	157.83			4.6	326	4.1	2.3	91.1	7.2				
19X-2, 135-150	164.53	16.7	0.87	4.2	294	10.1	5.7	91.0	3.0				
20X-4, 135-150	177.13			6.5	378	16.5	5.6	91.1	3.3				
21X-3, 135-150	185.23	24.7	1.11	11.0	326	21.8	3.7	92.8	2.9				
21X-4, 135-150	186.73			13.8	365	21.4	3.6	91.0	3.0				
21X-5, 110-125	187.98	23.9	1.28	12.4	382	21.4	4.0	88.8	1.5				
21X-6, 75-85	189.10	23.9	1.32	14.5	375	24.8	9.1	90.2	1.6				
22X-1, 88-103	191.36	24.3	1.36	17.4	359	26.5	4.7	90.1	2.0				
22X-2, 47-62	191.98	24.3	1.27	16.2	342	26.0	6.0	90.0	4.0				
168-1024A-													
1H-1, 115-125	1.20			58.4	520	126.0	22.9	85.9	1.0				
1H-2, 140-150	2.80			48.5	483	94.4	20.1	86.4	0.7				
1H-3, 140-150	4.30			39.2	491	64.5	20.8	86.2	0.7				
1H-4, 140-150	5.80			36.8		5.1							
1H-5, 140-150	7.30			40.3	495	51.9	17.2	83.5	0.9				
1H-6, 140-150	8.80			37.8	517	45.2	17.3	84.8	1.8				
168-1024B-													
1H-1, 140-150	1.45		1.84	55.9		92.8		87.9	0.6				
1H-2, 140-150	2.95	18.6	1.65	44.4	489	109.2	7.4	88.4	0.6				
1H-3, 140-150	4.45			35.1	513	85.6	4.8		4.0				
1H-5, 140-150	7.33	8.8	1.31	36.0	530	70.3	32.2	85.9	2.6				
2H-2, 140-150	10.55			26.7	520	57.8	11.4	82.5	1.3				
2H-5, 140-150	15.05	14.3	1.37	34.9	514	47.0	17.0	85.2	0.8				
3H-5, 140-150	24.55			26.3		41.3		83.3	0.8				
4H-5, 140-150	34.05	15.9	1.18	17.5	511	15.0	4.8	79.5	2.9				
5H-5, 140-150	43.55			9.3		0.7		79.4	3.5				
6H-5, 140-150	53.05	11.0	1.04	6.7		3.3		82.0	1.6				
7H-5, 140-150	62.55			4.2		9.3		79.5	2.5				
8H-5, 140-150	72.05	14.6	1.15	5.6		5.5		82.2	8.7				
9H-5, 140-150	81.55			5.1	406	13.3	4.7	96.4	45.7				
10H-5, 135-150	91.03	13.6	0.89	3.5	399	8.7	4.9	98.4	66.3				
11H-5, 135-150	100.53			3.4	362	9.2	6.0	95.3	61.1				
12H-5, 135-150	110.03	16.9	0.84	6.2		11.8		101.4	38.9				





Table 1 (continued).

Core, section, interval (cm)	Depth (mbsf)	Li (mmol/kg)	Rb (mmol/kg)	F (mmol/kg)	B ( $\mu$ mol/kg)	Mn (mmol/kg)	Fe (mmol/kg)	Sr ( $\mu$ mol/kg)	Ba (mmol/kg)	$^{87}\text{Sr}/^{86}\text{Sr}$	$\delta^{18}\text{O}$ (per mil)	$\delta\text{D}$ (per mil)	$\delta^{34}\text{S}$ (per mil)
17X-2, 130-150	142.90			5.5	428	26.6	2.9	179.3	6.8				
18X-2, 130-150	152.50	53.4	0.27	7.0	422	38.2	2.8	196.4	5.5		0.01	2.72	
19X-2, 130-150	162.10			6.7	391	32.5	3.4	205.2	3.3				
20X-2, 130-150	171.70	63.4	0.26	8.0	384	44.1	3.3	208.3	2.8		-0.03	1.93	
21X-2, 130-150	181.30			10.8	389	60.7	1.6	198.1	1.9				
22X-2, 130-150	190.90	69.4	0.28	13.9	324	70.9	2.6	199.2	2.3		-0.04	3.04	
22X-6, 130-150	196.90			15.7	300	73.2	2.1	194.9	2.3				
23X-2, 130-150	200.50	67.9	0.30	16.7	291	82.8	4.8	185.6	1.2		-0.13	1.15	
23X-6, 130-150	206.50	63.9	0.36	16.4	280	94.8	2.8	169.9	1.3				
24X-5, 125-150	213.10	56.4	0.50	22.2	197	67.9	4.0	155.3	1.5		-0.08	1.43	
24X-5, 125-150	214.60	54.0	0.36	18.4	227	98.2	4.2	156.4	1.9				
24X-6, 125-150	216.10	53.9	0.37	17.4	185	95.8	3.2	157.9	0.9		-0.05	3.35	
25X-1, 125-150	218.20	45.4	0.59	13.7	205	67.9	4.9	134.9	0.8				
25X-2, 125-150	219.70	42.8	0.60	14.3	205	80.3	2.9	136.5	2.8		-0.27	1.40	
168-1030B-													
1H-1, 140-150	1.45	20.3	1.97	38.5		61.8		93.4	0.6				
1H-2, 140-150	2.95	13.2	1.50	21.1	529		9.7	50.0	0.7				
1H-3, 74-84	3.79	12.1	1.58	15.8		43.6		100.1	0.5				
2H-1, 140-150	5.45	13.8	1.29	7.7	571	45.3	4.5	105.3	0.6				
2H-2, 140-150	6.95	15.7	1.42	8.9		46.1		107.2	0.8				
2H-3, 140-150	8.45	18.1	1.38	9.2	576	48.4	6.9	108.4	0.6				
2H-4, 140-150	9.95	21.9	1.23	9.5	514	51.6	7.6	108.0	0.6				
2H-5, 140-150	11.45	23.2	1.29	11.3		45.9		109.1	0.6				
2H-6, 140-150	12.95			10.8	500	52.6	15.1	108.5	0.5				
2H-7, 62-72	13.67	24.8	1.21	11.1		54.7		108.4	0.5				
3H-2, 140-150	16.45			10.1	555	58.4	9.1	107.8	0.8				
3H-4, 140-150	19.45	29.1	1.16	9.6		66.7		110.8	0.7				
3H-6, 140-150	22.45			11.8	477	80.5	4.1	109.0	0.9				
4H-2, 140-150	25.95	27.3	0.92	15.7		86.7		108.6	0.5				
4H-4, 140-150	28.95			17.2	468	81.8	7.2	109.9	0.6				
4H-6, 140-150	31.95	30.4	0.78	18.2		77.5		109.7	0.6				
5H-2, 140-150	35.45	28.9	0.90	20.3	424	58.3	1.6	110.4	1.1				
5H-4, 140-150	38.45			19.8		36.3		109.4	0.7				
5H-6, 140-150	41.45	24.6	0.72	18.0	412	37.9	3.3	110.1	0.7				
6X-CC, 0-20	41.65	22.6	0.69	17.1		31.8		109.1	0.7				
168-1031A-													
1H-1, 140-150	1.45	27.6	1.78	37.5	492	50.6	12.3	104.2	0.4	0.707997	0.05	1.74	
1H-2, 140-150	2.95	29.2	1.63	33.7	473	55.6	8.8	107.0	0.5	0.707783	0.19	2.01	
1H-3, 140-150	4.45	30.1	1.54	31.9	511	63.5	5.2	108.1	0.4	0.707661	0.19	0.80	
1H-4, 140-150	5.95	30.5	1.60	31.1	475	62.6	8.4	109.6	0.5	0.707621	0.32	1.59	
1H-5, 140-150	7.45	30.9	1.48	29.1	483	67.1	10.4	111.2	0.4	0.707526	0.37	1.61	
2H-2, 140-150	11.75	31.6	1.23	27.6	487	90.1	5.7	113.3	0.6	0.707499	0.34	3.48	
2H-5, 130-150	16.20	32.9	1.15	27.7	435	91.3	8.5	111.7	0.6	0.707474			
3H-5, 140-150	25.75	33.1	0.92	31.6	399	50.5	2.4	111.6	0.9	0.707448	0.08	1.70	
4H-2, 140-150	30.75	27.5	0.83	34.0	342	23.7	2.2	111.6	0.7	0.707473	-0.06	1.66	
4H-5, 140-150	35.25	21.2	0.78	21.1	353	26.7	1.6	111.6	0.8	0.707398	-0.09	2.74	
5H-1, 140-150	38.75	15.5	0.74	12.7	377	16.2	2.3	113.1	0.8	0.707350	-0.18		
5H-2, 140-150	40.25	12.5	0.74	8.4	329	9.0	0.7	114.5	0.7	0.707358	-0.17		
168-1032A-													
2R-1, 130-150	195.50	46.3	0.38	9.4	384	20.6	5.6	161.4	3.3				
3R-1, 130-150	205.10	47.2	0.37	8.2	360	16.1	4.6	182.2	9.9				
5R-2, 130-150	225.80			9.5	400	25.1	6.1	207.2	11.0				
6R-2, 130-150	235.40	51.1	0.27	12.2	371	41.3	2.1	198.9	4.9				
7R-2, 130-150	245.00			11.1	316	42.7	1.9	206.1	2.8				
8R-2, 130-150	254.60	51.7	0.28	15.1	270	28.0	5.4	194.9	5.3				
10R-1, 43-63	271.53	54.9	0.25	23.3	269	64.6	5.0	181.9	2.9				
10R-2, 88-108	273.48			23.6	237	71.1	5.9	180.7	0.8				
10R-3, 130-150	275.40	56.5	0.28	25.4	228	68.3	1.3	179.9	1.5				
10R-4, 30-50	275.90	50.7	0.31	37.3	161	30.6	1.5	176.5	1.6				
11R-1, 130-150	282.00	47.1	0.24	29.9	202	99.0	0.2	169.0	1.3				
11R-2, 130-150	283.50			29.7	215	82.6	-0.2	166.2	1.1				
11R-3, 130-150	285.00	28.0	0.26	23.2	156	20.3	2.2	156.4	1.0				

Notes: \* = aliquot from overflow chamber; values have been corrected to the chlorinity of the prime aliquot, from the titanium coil. † = trace element data from Wheat and Mottl (2000); Sr isotopic data from Butterfield et al. (in press).

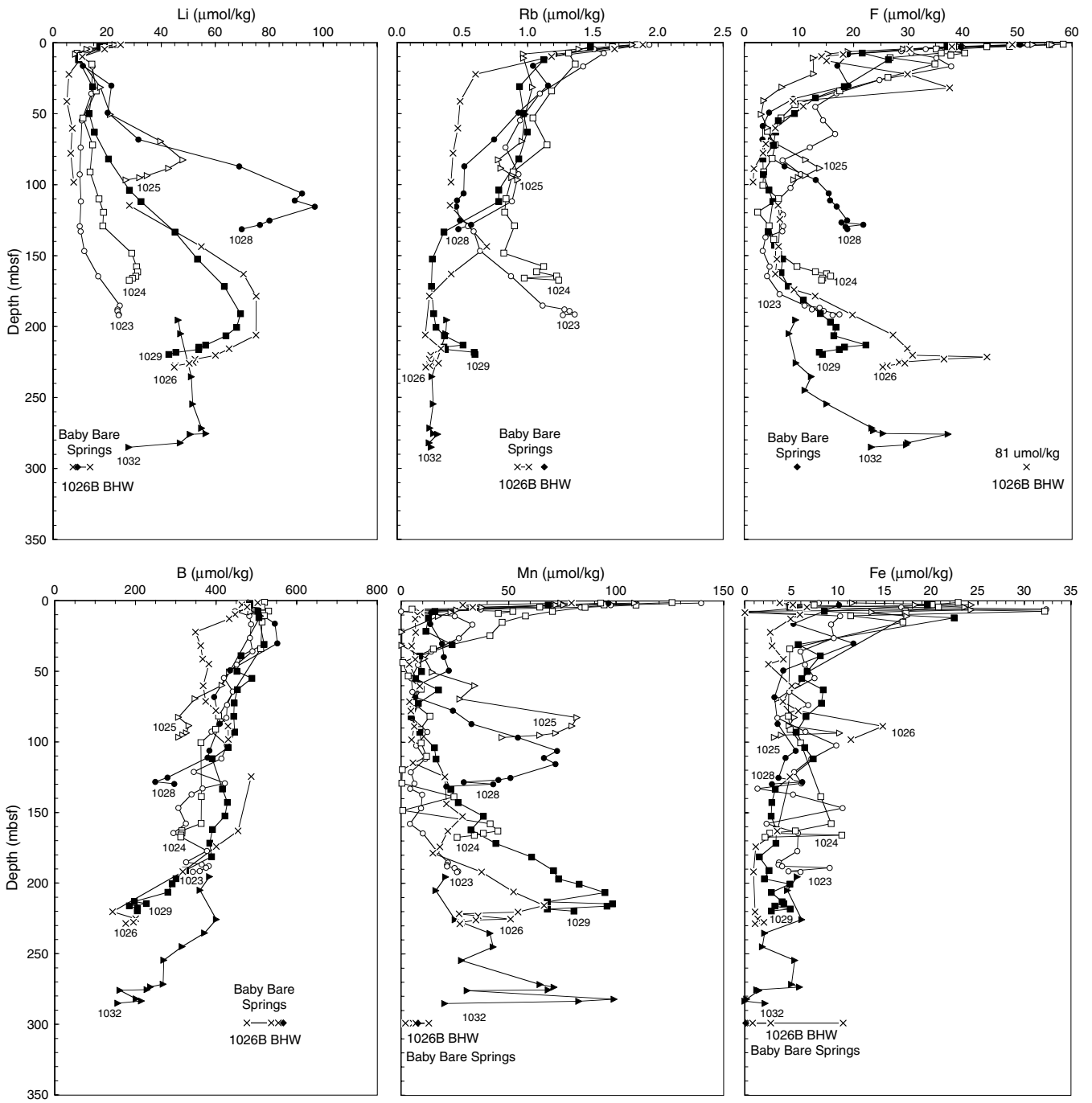


Figure 1. Composition of pore water from cores at Sites 1023 (open circles), 1024 (open squares), 1025 (open triangles), 1026 ( $\times$ 's), 1028 (solid circles), 1029 (solid squares), and 1032 (solid triangles), compared with water sampled from 256 m depth within the basement section of the open borehole in Hole 1026B ( $\times$ 's at bottom) and with spring waters sampled from Baby Bare summit (diamonds). BHW = borehole water.

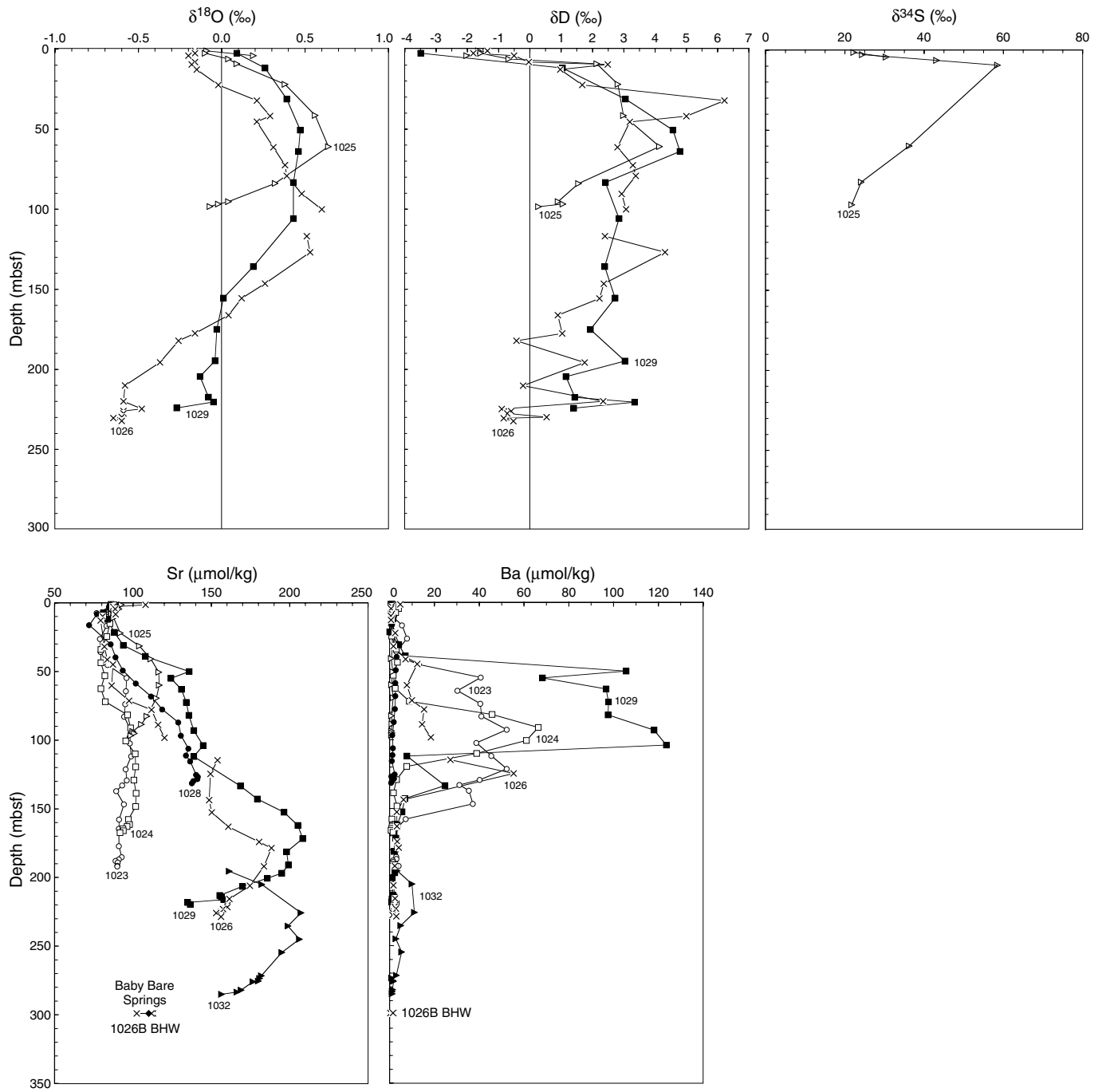


Figure 1 (continued).

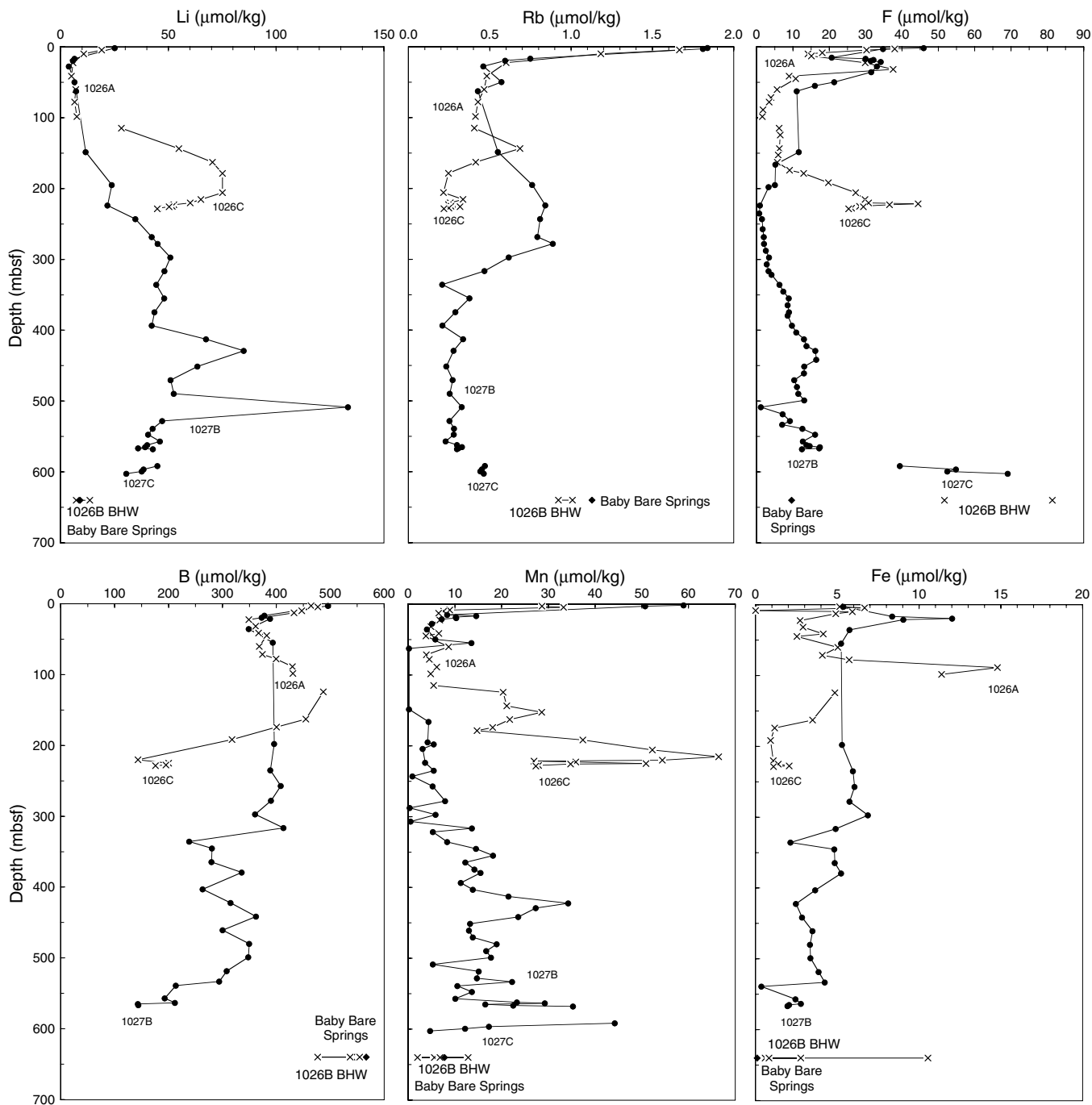


Figure 2. Composition of pore water from cores at Sites 1026 (x's) and 1027 (solid circles), compared with water sampled from 256 m depth within the basement section of the open borehole in Hole 1026B (x's at bottom) and with spring waters sampled from Baby Bare summit (diamonds). BHW = borehole water.



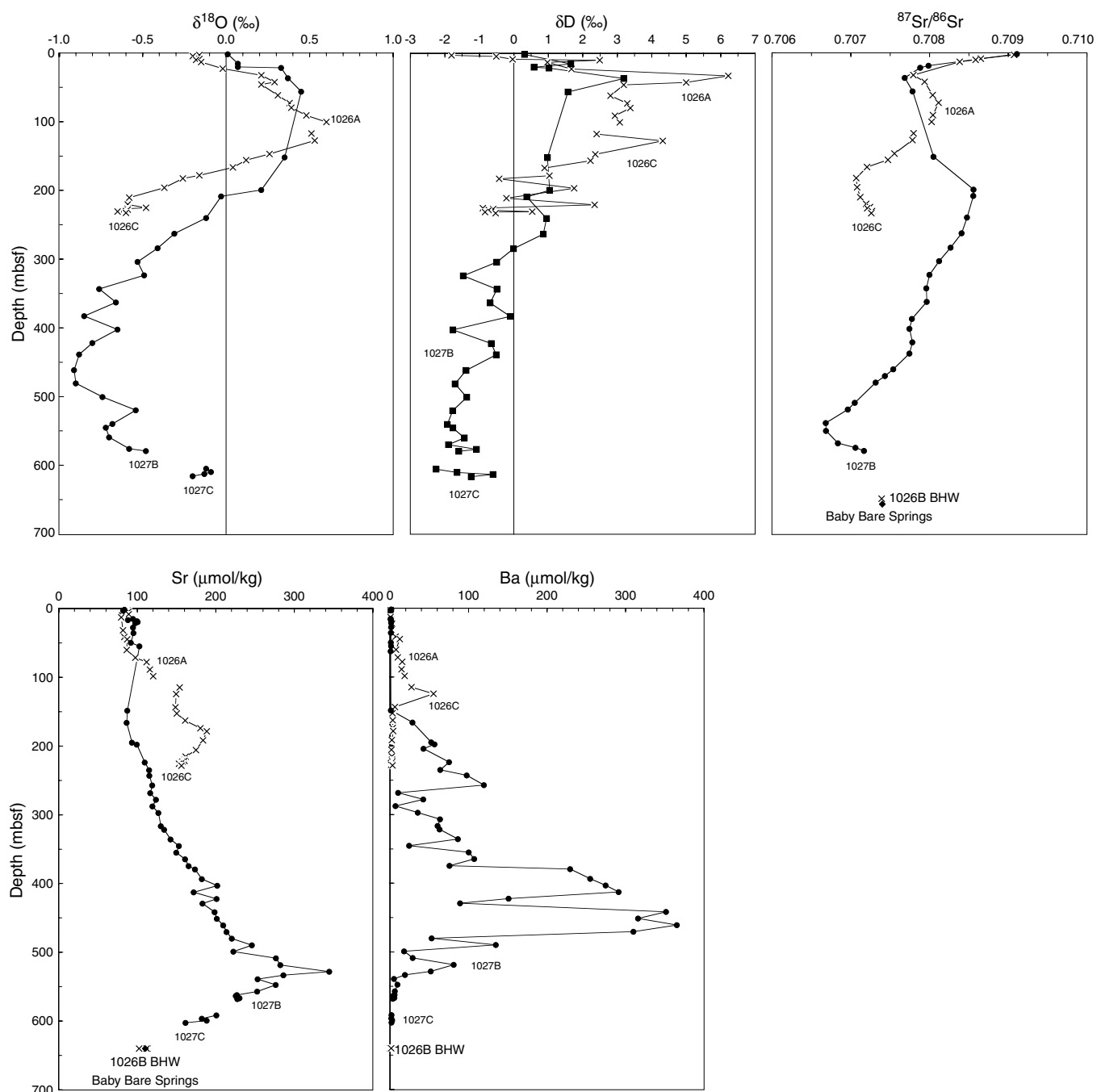


Figure 2 (continued).

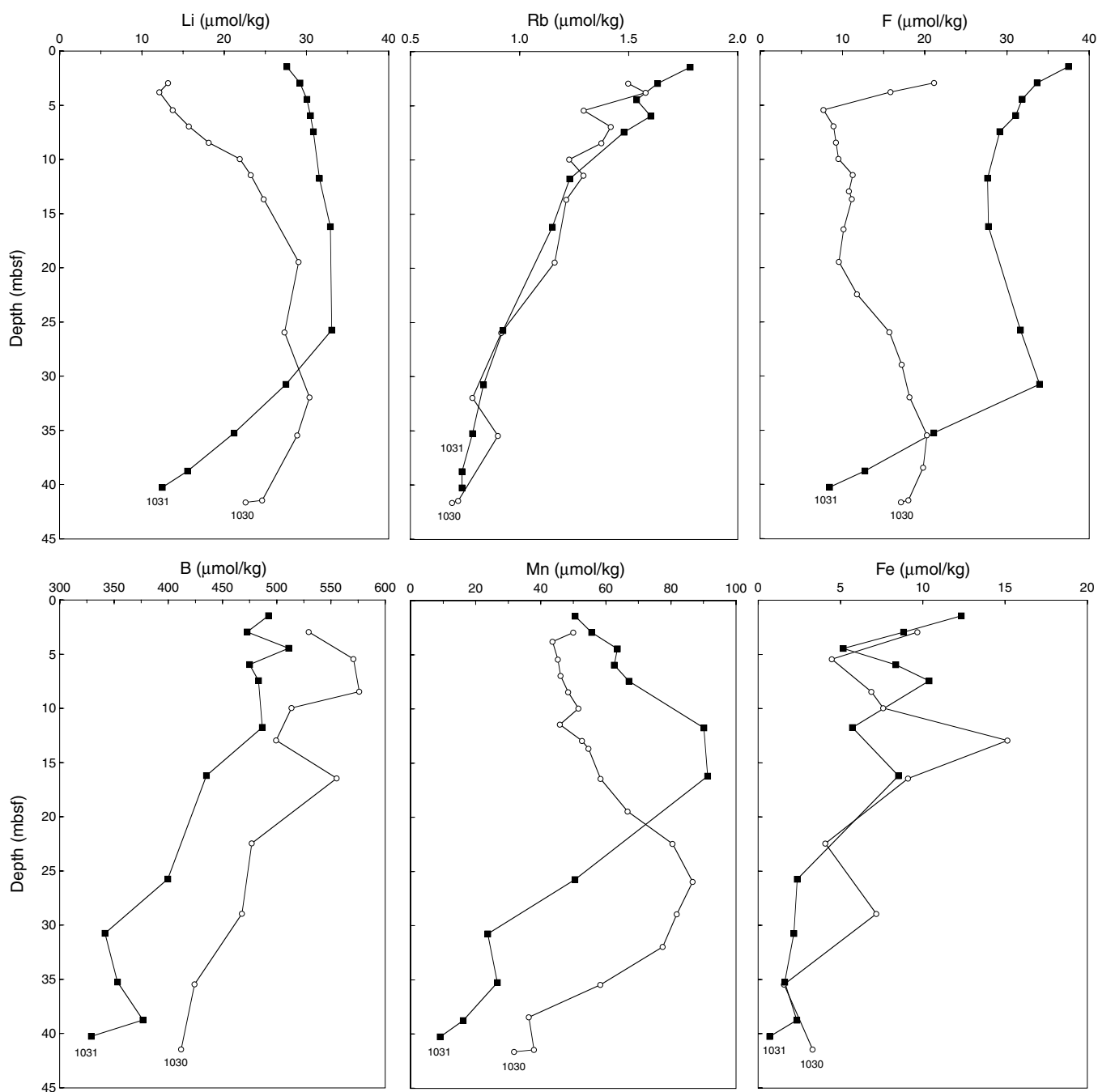


Figure 3. Composition of pore water from cores at Sites 1030 (open circles) and 1031 (solid squares).

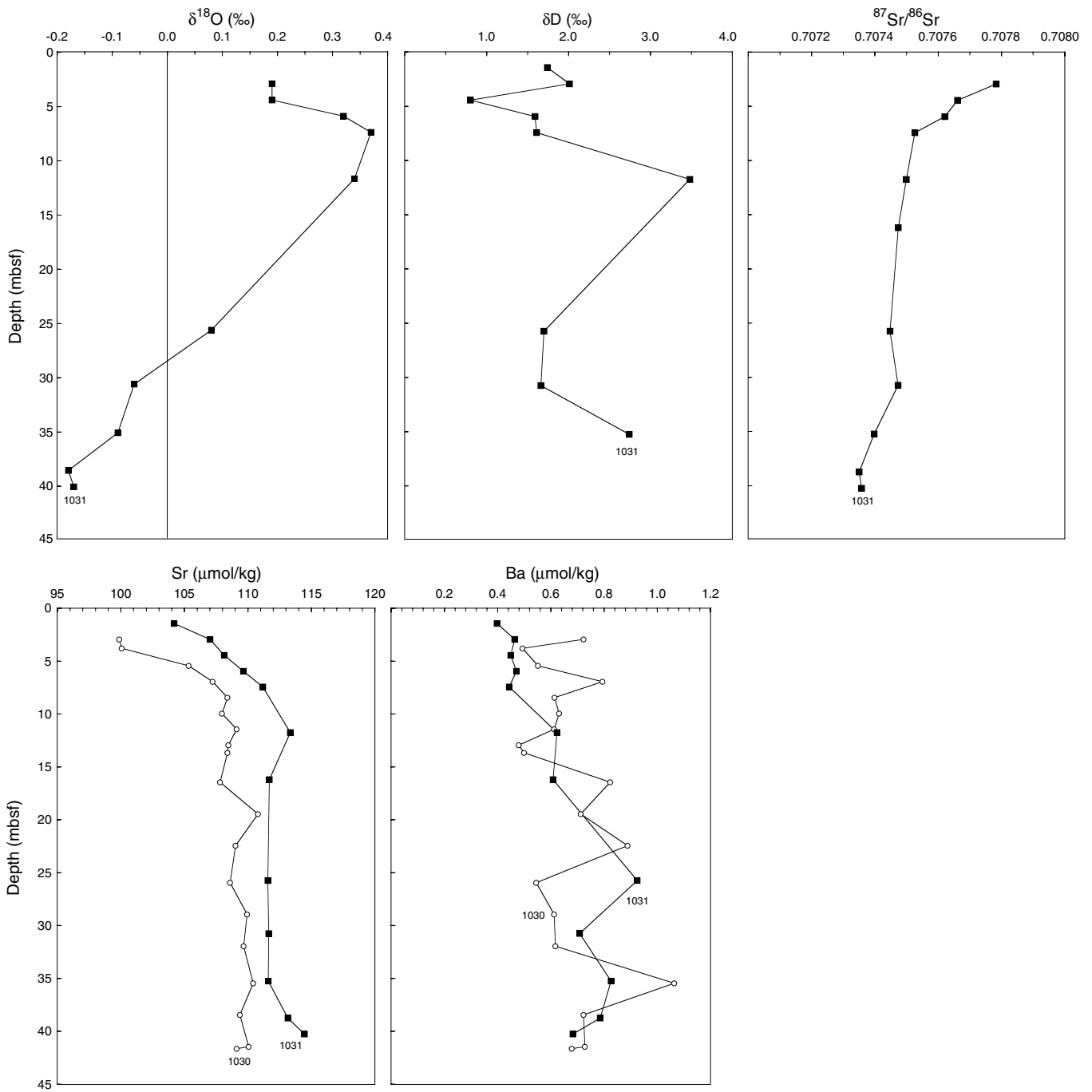


Figure 3 (continued).